 SDHM, vol.4, no.2, pp.53-65, 2008

A Study of Damage Identification and Crack Propagation in Concrete Beams

A. Brasiliano[1], W.R. Souza[2], G.N. Doz[3] and J.L.V. Brito[4]

Abstract: It can be observed that usually, during structures useful life they are submitted to deterioration processes that, depending on the intensity, may affect their performance and load capacity and, as a result, their safety. In this case, it is necessary to accomplish an inspection in order to evaluate the conditions of the structure and to locate and quantify the intensity of the damage. Another important point is to study the behavior of brittle material beams with cracks, as an attempt of understanding the rupture mechanism and crack propagation phenomenon. In this paper, the Residual Error Method (Genovese, 2000) is applied to a concrete beam in order to identify and quantify damages in its structure. This method is based on the alteration produced by damage in the dynamic properties of structures. The results obtained by this method allowed to locate and to quantify damages in a beam. The phenomenon of crack propagation is studied by others methods too: the Fracture Mechanics approaches and the Discrete Element Method (DEM). Changes on the dynamic behavior, crack trajectories, peak loads and energy variations were observed during the simulation.

Keyword: Damage, dynamic properties, brittle materials, fracture mechanics, crack propagation.

1 Introduction

In general, the structures suffer deterioration processes during their useful life. These processes can be originated from corrosion phenomena, chemical attack, carbonation, radiation, among others. Besides these factors, the civil engineering structures are submitted to several types and forms of static and dynamic loads such as permanent or accidental loads, movement of people, vibration of machines, wind forces, earthquakes, impact, fatigues etc. The combination of load conditions and deterioration processes, depending on the intensity, can produce different types of structural damages.

This fact, obviously, results in a reduction in carrying capacity or a reduction in the structure's ability to control motions under imposed forces, and, in extreme cases, it can compromise the structures global stability. In this case, when there are doubts about the structural integrity, it is necessary to use certain techniques to evaluate the global conditions of the structure. This is important because if the damage is not identified, it can result in the rupture of some components and affect the performance of the structure, and, consequently, its safety.

Normally, the techniques used to evaluate these conditions require much time and money to be applied. Therefore, the development of cheaper and faster damage identification methods is very important. The damages that appear in a structure are normally characterized by a local loss of stiffness and mass, but the damage effect upon the stiffness is in an extent much greater than the one upon the mass. Then the loss of mass can be considered null as observed by Hearn and Testa (1991). The loss of stiffness can be expressed as a reduction in the geometrical and/or physical properties of the structural component. The latter may be caused by chemical processes implying in the reduction of the Young's Modulus.

The presence of damage in a structure causes changes in the modal parameters such as natural frequencies, mode shapes and modal damp-

[1] UFPE, Caruaru, PE, BRAZIL.
[2] UnB, Brasília, DF, BRAZIL.
[3] UnB, Brasília, DF, BRAZIL.
[4] UnB, Brasília, DF, BRAZIL.

ing values, as observed by several authors, such as Adams *et al.* (1978) and Chen *et al.* (1995). Depending on the location and severity of the damage the changes in the modal parameters may affect each mode differently, offering the possibility of detecting, locating and quantifying the damage (Adams *et al.*, 1978 and Salawu, 1997).

Many damage detection methods have been developed over the last years to locate and quantify damages using dynamic properties, for example, natural frequencies and mode shapes. Doebling *et al.* (1998) and Zou *et al.* (2000) present an interested and detailed review about this subject. In the present work, however, just some ideas by a small number of authors will be presented here.

Genovese (2000) developed a method to locate and quantify damages in structures based on the error that appears in the modal equation of the intact structure when, the frequencies and mode shapes of the damaged structure are used instead. The author made an experimental and numerical analysis of free-free beams. The damage identification was satisfactory for the most analyzed cases. Brasiliano (2001) and Brasiliano *et al.* (2004) also applied this method in other types of structures, continuous beams and frame structures, obtaining very good results in the location and quantification of the damage.

After that, Genovese (2005) applied the residual error method to a dynamic test simulation of a simple supported beam in order to verify its efficiency. The displacements versus time, produced by an impulsive load, were obtained at several points of the beam. A white noise signal with different levels was added to the obtained records in order to simulate a suitable dynamic test. The damage was simulated by the reduction of the geometric properties of the chosen element. It was observed that the noise affects the structural evaluation process, and difficult the correct localization and quantification of the damages region. It was also observed that, the process of location the damage is more efficient as compared to the quantification one. The correct damage detection depends, also, on the location and severity of the damage.

Abdo and Hori (2002) presented a numerical study of the relationship between damage characteristics and the changes in the dynamic properties. In their studies, they verified that the rotation of mode shapes was a sensitive indicator of damage and the results showed that this rotation has the characteristic of localization at the damaged region even though the displacements modes are not localized.

Ndambi *et al.* (2002) presented experimental results obtained within the framework of the development of a health monitoring system for civil engineering structures, based on the changes of dynamic characteristics. The authors subjected reinforced concrete beams to cracking processes. The cracks were introduced in different steps and the damage assessment consisted in relating the changes observed in the dynamic characteristics and the level of the crack damage. It was observed that the eigenfrequencies were affected by accumulation of cracks in the beams.

Besides locating and quantifying damages, it is important to know which factors can contribute to a structure collapse. This can be done, for example, by studying the behavior of structures that have cracks or discontinuities. One of the possible tools that allow this analysis is the Fracture Mechanics that gives the fundamental rules about crack propagation. In addition, the combination of numerical methods, such as the Finite Element Method (FEM), the Boundary Element Method (BEM) and the Discrete Element Method (DEM), make it possible to apply it to complex cases.

The Finite Element Method and the Boundary Element Method can be used with accuracy to solve various types of problems including those with physical and geometrical non-linearity. Nevertheless, there are some restrictions related to the application of these methods in the analysis of crack propagation problems in which the continuum theory is not valid anymore.

With the search of new models it will be possible to capture the conditions that may start the crack propagation and represent the behavior of the propagation process, including the possible cases of crack derivations and, thus, stop the crack growth. In this aspect, the Discrete Element Method has been producing good results.

The initial application of Fracture Mechanics consisted of studying the instability of the rupture mechanism of brittle materials. Its applicability, however, increased with the advance of the researches and, nowadays, it can be applied to various types of materials and structures. The first successful analysis about the fracture problem is assigned to Griffith's works related to crack propagation in glass. Griffith (1921) developed the idea that a crack in a plate would grow if the rate of the elastic energy stored in the plate became equal or exceeds the work necessary to produce a fracture surface. His theory permits to state the quantitative relation between the material resistance and the crack size, establishing a rupture criterion, the energetic criterion. When his model was applied to ductile materials, such as metals, however, the results were not satisfactory. In order to become the Griffith's theory applicable to ductile materials, Irwin (1958) proposed an alteration in this theory and established the Generalized Griffith's Model.

In the 60's, many researches were carried out as an attempt to find a criteria of analysis that would make it possible to represent the non-linear behavior of some materials. Since Kaplan (1961) applied the Linear Elastic Fracture Mechanics (LEFM) to investigate cracked beams, the fracture in brittle materials, such as concrete, became an important subject. Many features of brittle materials have been tested to validate the linear elastic fracture mechanics as a tool for studying cracks, such as the geometry of different structural elements, cracks length and compressive and tensile strength. In the 80's several shapes were proposed to evaluate the crack propagation and fracture in brittle materials which were submitted to combined tension and shear forces. This type of load is associated to strains in the tip of the crack and it is named mixed-mode of rupture (Swartz and Taha, 1991).

Many experiments were realized in order to explain the rupture of concrete structures. Among others, the works of Bazant *et al.* (1987), Bazant and Kazemi (1989), Raghu Prasad *et al*. (2000) and Cervenka *et al*. (2002) can be cited. In the 90's the fracture mechanic was extended to other research fields such as determination of the minimum reinforcement in concrete structures (Bosco *et al.* 1990), the study about fracture of structural elements submitted to dynamic loads (Du *et al.* 1992), crack propagation in simple and reinforced concrete structures (Saleh and Aliabadi, 1998), etc.

Because of the importance of damage identification methods based on the alteration in the dynamic characteristics of the structures to explain the behavior of damaged structures constructed with brittle materials, such as concrete, this paper shows a numerical study about asymmetric damages in beams submitted to three-point bend test. This example consists of two parts: in the first one, a verification of structural integrity of a simple supported beam is done. The beam is discretized in finite elements and damages are introduced in it by an inertia reduction of its elements. The Residual Error Method (Genovese, 2000, 2005) is applied in order to locate and quantify these damages. In the second part the damaged beam is submitted to a load scheme and the crack propagation phenomenon is studied based on the Linear Elastic Fracture Mechanics approach using the Discrete Element Method.

2 Description of the Residual Error Method

The residual error method proposed by Genovese (2000) is used to identify damages in structures. The identification is done in two steps: the location and quantification of the damage. The location is done by observing the error present in the modal equation, Equation (1), when the stiffness and mass matrices of the intact structure and the modes and natural frequencies of the damaged structure are used:

$$\mathbf{E} = \mathbf{K}\Phi' - (\mathbf{M}\Phi')\Lambda' \tag{1}$$

in which $\mathbf{K}$ and $\mathbf{M}$ denote, respectively, the stiffness and the mass matrix of the intact structure, Φ' is the matrix of the identified damaged mode shapes, Λ' is the diagonal matrix of natural frequencies of the damaged structure and $\mathbf{E}$ is the error matrix in which the values represent the error produced by damage in the modal equation.

$$\mathbf{E} = \begin{bmatrix} e_1 & e_2 & e_3 & \dots & e_n \end{bmatrix}_{N\times n} \tag{2}$$

$$\Phi' = \begin{bmatrix} \phi'_1 & \phi'_2 & \phi'_3 & \dots & \phi'_n \end{bmatrix}_{N\times n} \tag{3}$$

$$\Lambda' = \begin{bmatrix} \omega'^2_1 & 0 & 0 & \dots & 0 \\ 0 & \omega'^2_2 & 0 & \dots & 0 \\ 0 & 0 & \omega'^2_3 & \dots & 0 \\ \vdots & \vdots & \vdots & \ddots & \vdots \\ 0 & 0 & 0 & \dots & \omega'^2_n \end{bmatrix}_{n\times n} \tag{4}$$

where N is the number of spatial test points, n is the number of identified modes and ϕ'_i is the ith mode shape vector of the damaged structure.

Each column of matrix $\mathbf{E}$ is a vector that is related to one mode shape, Equation (2). Each value of this vector represents the error that occurs in some positions of the structure. Thus, the highest error value will indicate the damage position to a mode shape.

The damage quantification consists in looking for the minimum error in the modal equation by an iterative process. In this step it is introduced a factor p that will multiply only the stiffness matrix of the damaged element, which has been located during the previous step, before the global stiffness matrix of the structure be assembled. This step is showed schematically by Equation (7).

Considering that the damage will affect the stiffness in a much greater intensity than it will affect the mass (Adams *et al.* 1978 and Hearn and Testa, 1991), the factor p will multiply only the stiffness matrix. The iterative process consists in varying the value of p between 0 and 1 in order to obtain the minimum norm of the matrix $\mathbf{E} = f(p)$, Equation (5), in this interval.

$$E(p) = \mathbf{K}''(p)\Phi' - (\mathbf{M}\Phi')\Lambda' \tag{5}$$

where:

$$\mathbf{K}''(p) = \mathbf{K}_{\text{intact elements}} + p\mathbf{K}_{\text{damaged elements}} \tag{6}$$

or, schematically

$$\mathbf{K}''(p) = \begin{bmatrix} k_{EI} & & & \\ & k_{EI} & & \\ & & 0 & \\ & & & k_{EI} \end{bmatrix} + p \begin{bmatrix} 0 & & & \\ & 0 & & \\ & & k_{ED} & \\ & & & 0 \end{bmatrix} \tag{7}$$

where k_{EI} and k_{ED} represent, respectively, the stiffness matrix of the intact and damaged elements.

This method can be part of a structural health monitoring system where the dynamic properties are continuously determined by modal testing using reliable system identification techniques. The first step would be the verification of the structural integrity observing changes in the natural frequencies. If these changes indicate the presence of any damage, the residual error method could be used to locate and quantify it.

In this sense it is important to emphasize the necessity of performing modal testing before the structures being put on service because, this way, one can obtain the dynamic properties of these intact structures.

3 Discrete Element Method

The Discrete Element Method (DEM) is based on the representation of the continuous medium by an arrangement of cubic cells, like space truss with lumped nodal mass. Originally, this arrangement was used in aerospace engineering in order to perform structural analysis of truss systems that would represent, in an equivalent form, the continuous properties (See Nayfeh and Hefzy (1978) for details). Using an inverse approach, Hayashi (1982) obtained, from an isotropic elastic solid, the equivalent properties of each bar of the cell arrangement. This representation plays an essential role in the use of DEM. Fig. 1 shows details of cubic cell geometry and an example of a body constructed by using cell arrangements.

The diagonal bars length is $L_c\sqrt{3}/2$ and the normal bar's length is L_C. The parameter L_C is the

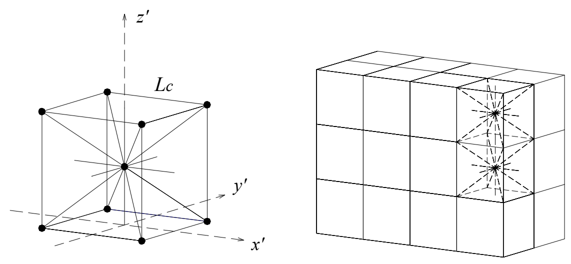

a) b)

Figure 1: a) Cubic module; b) Generation of a prismatic body using cubic module.

critical length which depends on the S-wave velocity and the maximum vibration frequency. In accordance with Hayashi (1982), for an isotropic and linear elastic material, with known Young's modulus (E) and Poisson's coefficient (ν), the equivalent stiffness of diagonal and normal bars is represented by equations (8) and (9), respectively:

$$E_d = \frac{2\delta}{\sqrt{3}} E_n \tag{8}$$

$$E_n = \alpha E L_C^2 \tag{9}$$

where α and δ are parameters of cubic truss model and are represented by equations (10-a and 10-b):

$$\alpha = \frac{9+8\delta}{18+24\delta} \tag{10a}$$

$$\delta = \frac{9\nu}{4-8\nu} \tag{10b}$$

The dynamic analysis is performed using an explicit integration in the time domain. At each step of integration, the following nodal equilibrium equation (11) is solved:

$$m\ddot{u}_i + c\dot{u}_i = f_i \tag{11}$$

where m represents the nodal mass, c is the damping constant, f_i are components of resultant forces at the node I, including elastic, external and frictional forces, and u_i are the components of nodal vector coordinates.

An explicit scheme of integration, based on central differences, is particularly useful, since it represents the nonlinearity aspect of the problem. Thus, the position of each particle at a specific moment $t+\Delta t$ is given by the following equation:

$$u_{i+1} = f_i \frac{(\Delta t)^2}{m} + 2u_{i+1} - u_{i-1} \tag{12}$$

where u_{i+1}, u_i and u_{i-1} denote the nodal positions at moments $t+\Delta t$, t and $t-\Delta t$, respectively.

The stability of the numerical integration is assured once the step size is bounded above by the critical value given by $0.6L_C/C_o$, that is:

$$\Delta t_{crit} \leq 0.6 L_C / C_o \tag{13}$$

where C_o represents the velocity of P-wave propagation and L_C is the bar's critical length.

Once the solid is represented by bars arrangement it is possible to easily treat complex problems. In this way, large displacements can be considered, in an efficient manner, since the nodal coordinates are changed at every time step. Hayashi (1982) verified the convergence of solutions obtained with discrete element method (DEM) in linear elasticity, as well as in elastic instability problems. Afterwards, Rocha (1989) extended the Hayashi's model (1982) to the analysis of fracture problems. Initially, the extension of the model to the study of linear elastic fracture mechanics problems was based on the idea that, as fracture takes place, the dissipated energy is proportional to the newly generated surfaces. Thus, the so-called Hilleborg model (see Fig. 2) is adopted as an effective uniaxial stress-strain curve for each individual element (Riera and Rocha, 1991). Observing this figure, it can be noticed that once the limit strain ε_r is reached, a given amount of energy is liberated. This energy equals the product of the fractured area A_f and the specific fracture energy G_f. It is important to notice that the fractured area (A_f) depends on the correlation length L_C of the process and that the fracture energy is a intrinsic property of the material.

The Discrete Element Method was also used to suitably represent the propagation of a seismic fault (Doz and Riera, 2000, Gudiel, 2000 and Gudiel et al, 2003), the size effect in concrete structures (Rios and Riera, 2002) and the behaviour of reinforced concrete structures submitted to short duration loading (Iturrioz, 1995 and Rios and Riera, 2002).

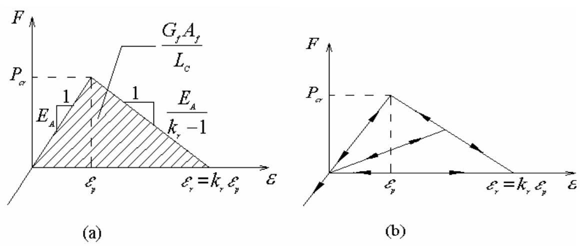

Figure 2: a) Constitutive diagram adopted; b) Loading and unloading scheme (Rocha, 1989).

The symbols in the diagram above mean: F is the axial force in the bar, it is function of deformation ε and P_{cr} is the value of this force associated with ε_p; E_A is the axial stiffness of the bar, it may be E_n or E_d if the bar is normal or diagonal respectively; ε_p is the critical rupture deformation, it is the deformation in which the crack becomes instable and starts to propagate. The properties ε_p, E, F and G_f depend on the material, A_f and L_C depend on the model and k_r and E_A depend on the material as well as the model.

The area under the diagram is proportional to the influence surface for the element under consideration. For the longitudinal bars:

$$\int_0^{\varepsilon_r} F(\varepsilon)d\varepsilon = \frac{G_fA_f}{L} \tag{14}$$

The performance of the Discrete Element Method applied to fracture problems was initially evaluated by reproducing some examples found in the literature. Among these, the concrete beam studied by Petersson (1981) can be cited. The results obtained by the Discrete Element Method were satisfactory and similar to those obtained by Petersson (1981) using Finite Element Method and by Saleh and Aliabadi (1998) using the Boundary Element Method (Souza, 2001). In the same way, the concrete beam studied by Bosco et al (1990) through an experimental and numerical analysis using the Finite Element and Boundary Element methods was also evaluated using the Discrete Element Method. The latter allowed to suitable simulate the after crack behavior in a more properly way than those methods aforementioned. It is important to highlight that just the Discrete Element Method allowed to simulate and analyze the dynamic aspects of rupture process.

4 Numerical analysis

4.1 Damage location and quantification by Residual Error Method

Simple Supported Beam

The Residual Error Method was applied to locate damage in one 2.4m long concrete beam with a rectangular cross-section of 0.14×0.24m. This beam was modeled with 24 equal elements of 0.10m in length. Every node has three degrees of freedom, a transverse displacement, an axial displacement and a rotation. The properties of the beam are: cross-sectional area A = 0.0336 m^2; moment of inertia $I = 1.6128 \times 10^{-4}$ m^4; Young's modulus $E = 3.5 \times 10^{10}$ N/m^2; density ρ = 2500 kg/m^3. The stiffness and mass matrices of the elements used to obtain the natural frequencies and mode shapes are defined by equations (15a and 15b).

Three damage cases were analyzed and the damaged elements are showed in Figure 3. The damages were introduced by a reduction in the inertia and the area of the elements and these values are summarized in Tab. 1. The natural frequencies of the intact and the damaged beam are showed in Tab. 2 and the first five mode shapes are showed in Fig. 4. In this case only numerical data were used in order to show the method application. In a real case the frequencies and mode shapes should be identified from experimental data obtained by dynamic tests.

$$k = \begin{bmatrix} \frac{EA}{L} & 0 & 0 & \frac{-EA}{L} & 0 & 0 \\ 0 & \frac{12EI}{L^3} & \frac{6EI}{L^2} & 0 & \frac{-12EI}{L^3} & \frac{6EI}{L^2} \\ 0 & \frac{6EI}{L^2} & \frac{4EI}{L} & 0 & \frac{-6EI}{L^2} & \frac{2EI}{L} \\ \frac{-EA}{L} & 0 & 0 & \frac{EA}{L} & 0 & 0 \\ 0 & \frac{-12EI}{L^3} & \frac{-6EI}{L^2} & 0 & \frac{12EI}{L^3} & \frac{-6EI}{L^2} \\ 0 & \frac{6EI}{L^2} & \frac{2EI}{L} & 0 & \frac{-6EI}{L^2} & \frac{4EI}{L} \end{bmatrix} \tag{15a}$$

$$M = \begin{bmatrix} \frac{1}{3} & 0 & 0 & \frac{1}{6} & 0 & 0 \\ 0 & \frac{13}{35} & \frac{11}{210L} & 0 & \frac{9}{70} & \frac{-13}{420L} \\ 0 & \frac{11}{210L} & \frac{1}{105L^2} & 0 & \frac{13}{420L} & \frac{-1}{140L^2} \\ \frac{1}{6} & 0 & 0 & \frac{1}{3} & 0 & 0 \\ 0 & \frac{9}{70} & \frac{13}{420L} & 0 & \frac{13}{35} & \frac{-11}{210L} \\ 0 & \frac{-13}{420L} & \frac{-1}{140L^2} & 0 & \frac{-11}{210L} & \frac{1}{105L^2} \end{bmatrix} \tag{15b}$$

The obtained results in the three damaged cases studied are showed in Fig. 5. In order to improve

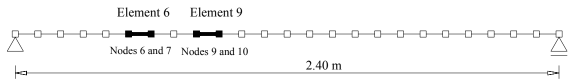

Figure 3: Simple supported beam with damage in elements 6 and 9.

Table 1: Reduction values of the inertia and area of the elements.

Cases Considered	*Elements*	*Inertia Reduction*	*Area Reduction*
Intact	—	0%	0%
1	9	10%	3.45%
2	9	40%	15.66%
3	6	50%	20.63%

Table 2: Natural frequencies of the intact and damaged beams.

Freq. (Hz)	*Intact*	*Case 1*	*Case 2*	*Case 3*
1^a	68.4992	68.3251	67.3814	67.5529
2^a	273.9975	273.4590	270.6865	266.1158
3^a	616.5024	616.4062	615.9045	605.0347
4^a	1096.0431	1092.9518	1077.9795	1093.6401
5^a	1712.6942	1710.3924	1699.7493	1702.5623

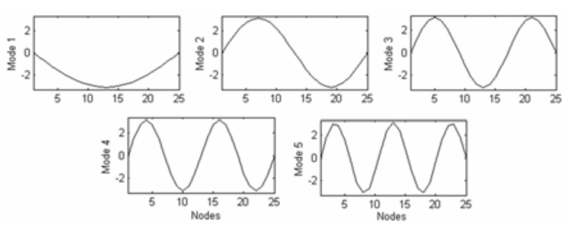

Figure 4: First five mode shapes of the intact beam.

the results, i.e., making the location of the damage more evident, a methodology of multiplying the error functions, obtained for the five modes, was used. Observing the Fig. 5, it may be verified that the results allow to identify the exact damaged elements using the first five mode shapes. This is evident because the largest peaks appear at nodes 9 and 10 for the first and second cases, 6 and 7 for the third case. These nodes define the damaged elements. The errors related with the axial and vertical degrees of freedom are not presented in the graphics because the multiplication of these values for the five modes was almost zero.

The values of inertia reduction initially considered and the values obtained by Residual Error Method are summarized in Tab. 3. The damage quantification was done using Equation (5) and, as it is showed below, the values of the factor p that produced the minimum norm of the matrix $\mathbf{E} = f(p)$ indicate an inertia reduction equal to the one initially considered. Actually, the inertia reduction is given by (1-p).

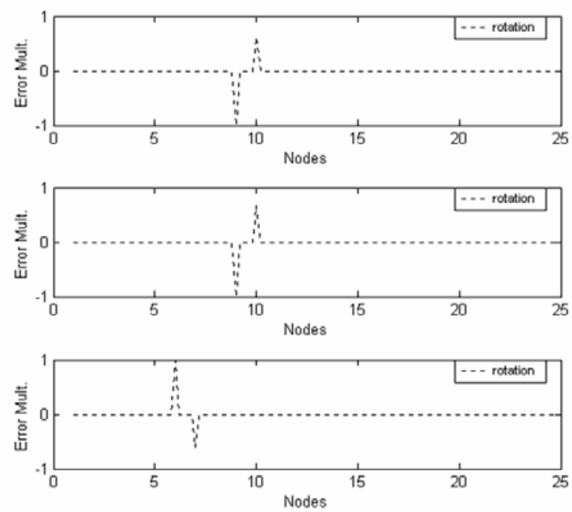

Figure 5: Damage location by Residual Error Method – Cases 1, 2 and 3 respectively.

Table 3: Inertia and area reduction introduced in the damaged elements, factor p and stiffness reduction obtained by the Residual Error Method.

Element	*Inertia Reduction Introduced*	*Area Reduction Introduced*	*Factor p*	*Stiffness Reduction $(1-p)$*
6	50%	20.63%	0.50	50%
9	10%	3.45%	0.90	10%
9	40%	15.66%	0.60	40%

4.2 Crack Propagation Analysis

In this stage the crack propagation phenomenon will be studied by a numerical analysis. The analysis will be done by observing the behavior of the beam, considering the aforementioned damage cases.

Numerical Simulation using the Discrete Element Method

Fig. 6-a and 6-b shows the geometric characteristics of the beam without damage and the load scheme. The physical properties of the material used to simulate the testing are summarized in Tab. 4. The value of specific energy of fracture G_f was calculated according to CEB-90. A coefficient of variation (CVA) for the fracture energy and the Young's modulus was adopted to simulate the non-homogeneous behavior of the material. This value is also showed in Tab. 4.

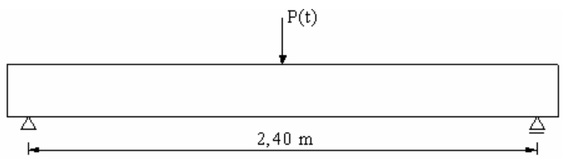

(a)

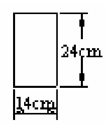

(b)

Figure 6: Geometric characteristics of the intact beam.

Table 4: Parameters adopted to generate the numerical model.

Properties	*Values*
Specific fracture energy, G_f	135 Nm^{-1}
Poisson's coefficient (ν)	0.20
Fail factor, R_f	1.5776 $\mathrm{m}^{-1/2}$
Damping rate (ξ)	5%
Coefficient of variation, CVA	0.10
Bars length, L_C	0.05 m
Young's modulus, E	3.5×10^{10} $\mathrm{N/m^2}$

Tab. 5 shows the models of the beam with the three damaged cases. The position of the initial crack from the left support of the beam was 0.80m, 0.80m and 0.50m for cases 1, 2 and 3, respectively. The inertia reduction considered for each case was 10%, 40% and 50%, respectively. The initial crack is 0.10m in length. The models of the beam were divided in $48 \times 5 \times 3$ modules in the x, y and z direction, respectively (Souza, 2001).

Table 5: Models of the beam with damage at different positions and inertia reductions.

Modelling Schemes	Case
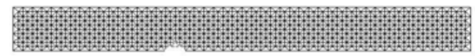	1
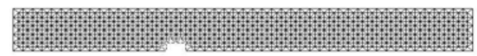	2
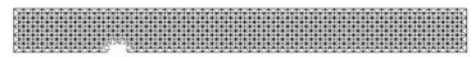	3

Considering the cases studied (Tab. 5), Fig. 7 shows the evolution of the load versus the displacement that occurs in the center of the beam. The load was applied in a quasi-static way without the control of the displacements, so it can be verified that the strains grow indefinitely when the rupture of the beam occurs. Comparing with the first case, it can be noticed a reduction in the reached ultimate load (nearly 20%) for the second case. This reduction is probably due to the size of the initial damage that is greater than that considered in the first case. In the third case, although it shows inertia reduction five times greater than the one considered in the first case, the value of the reached ultimate load was practically the same. This effect is probably due to the fact that the initial crack is located nearer the support and this region is submitted to predominant shear forces. Another fact that may have influenced these final results is the stress distribution in the beam.

The energy balance in the model during the numerical test was carefully monitored and the evolution of different forms of energy of relevance in the different rupture process is showed in Fig. 8. Once the control of the displacements was not being considered in this analysis, the external energy tends to grow indefinitely after the rupture. The potential elastic energy presents its maximum value of 6.55Nm at 0.132s, case 1, indicating the rupture of the beam since it is not able to absorb energy anymore. The fracture process begins at 0.11s appearing regions with micro cracks. The fracture energy grows smoothly until a plateau is reached at 0.137s.

The second case, compared to the first one, showed a reduction of 40% in the final values of

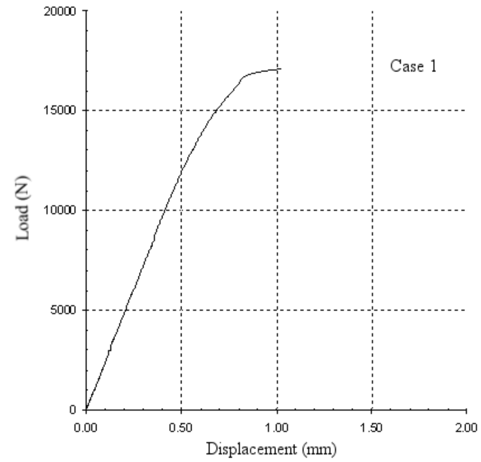

(a)

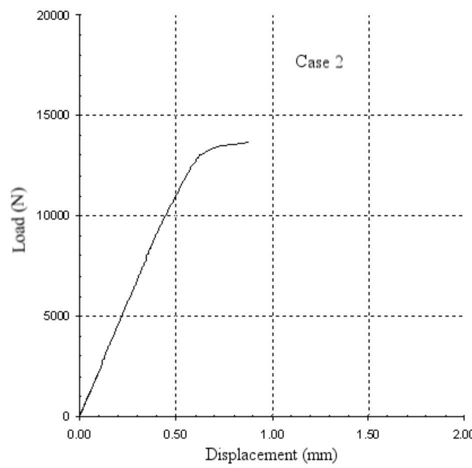

(b)

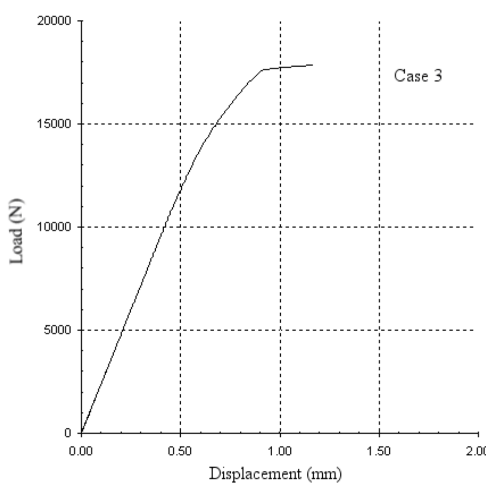

(c)

Figure 7: Load-Displacements in the center of the beam for the cases considered in the analysis.

the elastic and fracture energies due to the reduction of the ultimate load. This can be noticed comparing the values presented in Fig. 8. These energies also suffered changes for the third case. They show an increase of nearly 15% in relation to the first one.

Once the rupture process is a dynamic process, accelerations were induced into the solid. The use of the Discrete Element Method allowed the acceleration monitoring at any point of the mesh. Accelerations were obtained in the control points (Fig. 9) for the first and second cases. For convenience, only the results obtained from the point W_00 will be showed (case 1). Coordinates of the control points are summarized in Tab. 6.

Observing Fig. 10, which shows the results obtained for the first case, it can be seen that the accelerations that appears before the crack propagation starts are almost zero. The accelerations increase as the damaged regions increase and they reach peaks of nearly 10m/s^2 in x direction. For the other cases the same behavior was observed.

Table 6: Coordinates of points W_00, W_10, W_01 and W_11-considered cases.

	Cases 1 and 2		*Case 3*	
Points	X (m)	Y(m)	X (m)	Y(m)
W_00	1.20	0.00	1.20	0.00
W_10	0.60	0.00	0.30	0.00
W_01	1.10	0.00	0.80	0.00
W_11	0.85	0.10	0.55	0.10

Fig. 11 shows the crack propagation for the case 1. It can be observed that the concentration of tension forces, located at the middle of the beam, produces the first sign of damage. The resistance capacity of the beam was reached at the point where the initial crack was located. After that, the crack propagation initiates – with a tendency to increase – following an angle of nearly 45° in relation to the largest length of the beam (shear mode). It occurs until the instant 0.132s and then it goes up vertically (tension mode) indicating a mixed crack propagation. The mean propagation velocity was nearly 157 m/s in this case. The behavior of the damaged beam characterized by the second case was similar to the first one with a

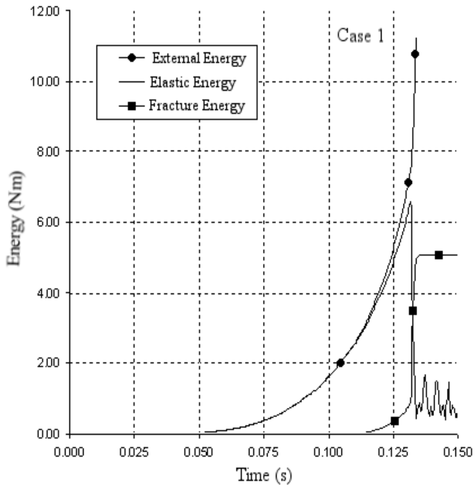

(a)

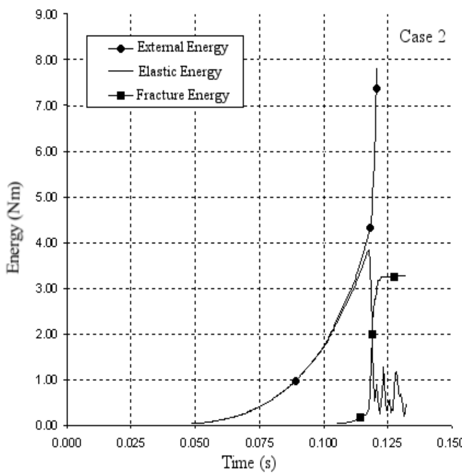

(b)

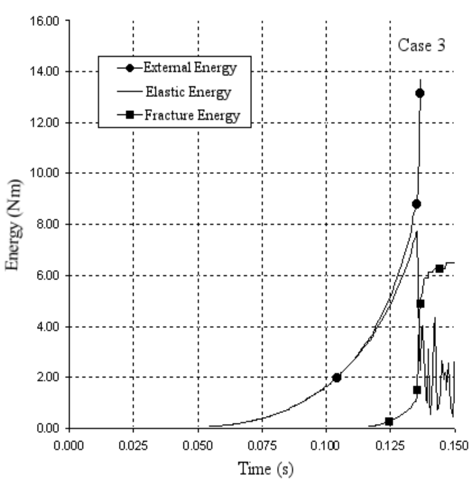

(c)

Figure 8: Energetic balance for the cases considered in the analysis.

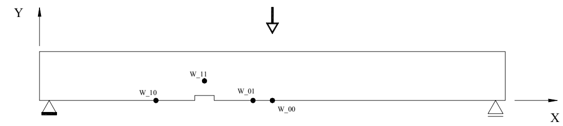

Figure 9: Control points of acceleration – Cases 1 and 2.

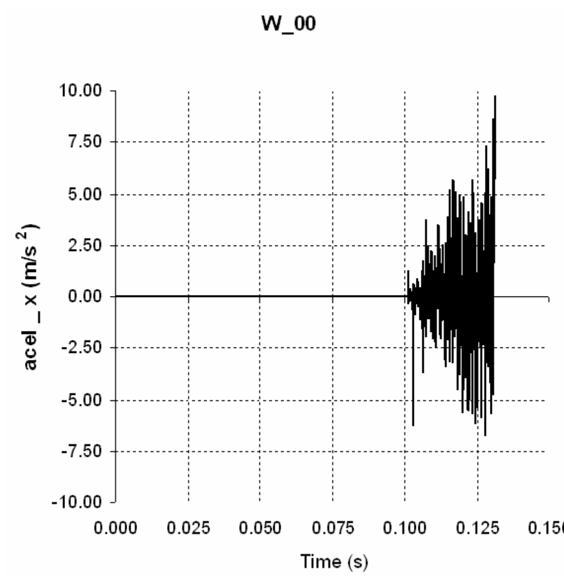

(a)

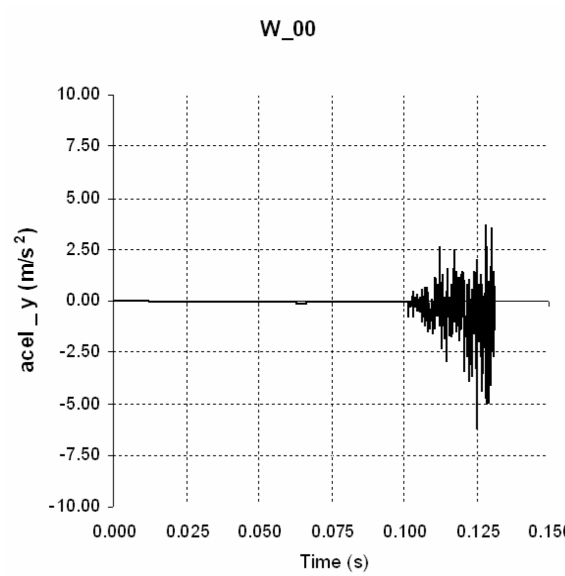

(b)

Figure 10: Accelerations in the x and y directions – control point W_00 – Case 1.

propagation velocity of nearly 62 m/s. In the third case, the observed behavior was different from the other two cases: there was a force concentration also around the initial crack and the more damaged region was located in the middle of the beam where the rupture occurs, as it can be seen in Fig. 12.

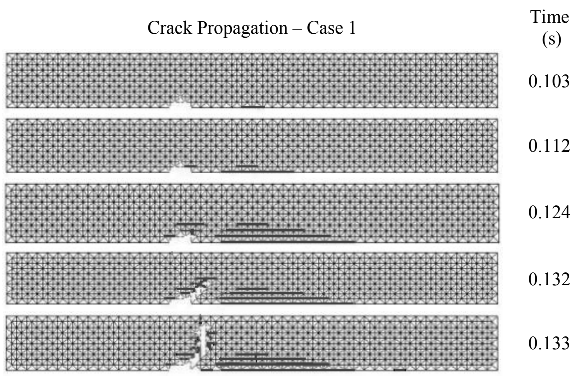

Figure 11: Crack propagation in the beam with a damage of 10% in the element 9 – First case.

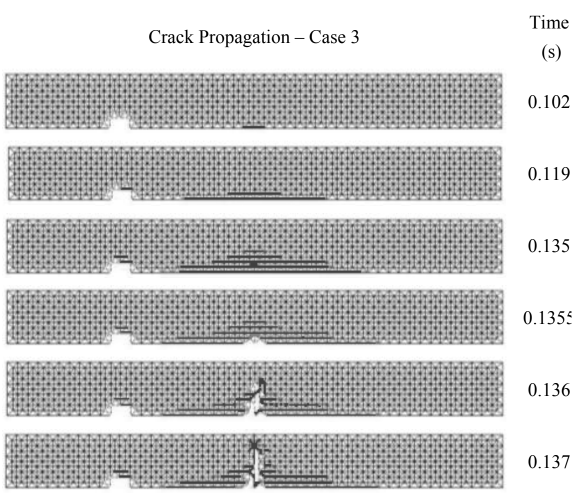

Figure 12: Crack propagation in the beam with a damage of 50% in the element 6 – Third case.

5 Conclusions

The Residual Error Method was very efficient in the damage identification of the considered structures allowing to locate and quantify the damages successfully. It is appropriate to point out that this paper presents a numerical analysis of computed structures but the residual error method can be applied to real structures since it is possible to obtain their modal parameters. The method intends to identify the damage location and its magnitude accurately, making necessary the measurements of the intact modal parameters. The perfect eigenmodes could be obtained performing modal testing in the new structure before it be put on service. If there is a continuous monitoring of the structure, changes in the modal parameters can be detected indicating presence of damage. In this way the method may also be used to measure the evolution of the damages. On the other hand, if it is impossible to obtain the intact natural frequencies and vibration modes, the method will compare the present measurements with a theoretical computed model of the intact structure. In that case, the analysis must be more careful because errors due to an incorrect model may be introduced in the problem.

About the crack propagation analysis, the obtained results indicated that the Linear Elastic Fracture Mechanics and the Discrete Element Method can be applied to this type of study. The shape and trajectory of the crack is meaningfully influenced by the initial crack position and by the load. It can be also concluded that the trajectory of the crack is associated to intense stress regions which are similar to tensile or strength testing of Lobo Carneiro (Brazilian test). When there is not geometry symmetry and the initial crack is located in regions that are submitted to preponderant shear forces, the relation between the modes I (tensile mode) and II (shear mode) of rupture produces mixed-mode crack propagation.

Three phases of the process can be observed. In the first one the beam was able to absorb almost all the energy imposed by the external load. In the second phase the beam capacity of absorbing energy was exceed and the fracture energy was produced. At this moment regions of microcracks appeared. The last one was the phase in which the crack propagation itself occurs.

Another aspect that was noticed is that the accelerations increase with the growth of the damaged regions and, in a parallel direction, they are greater than the cracks. Besides that, it could be observed that the accelerations before the propagation start are almost zero. It is also important to comment that the load was applied in such a way that the number of produced inertia forces was very small.

The results here obtained confirmed that the instable crack propagation constitutes an essentially dynamic phenomenon.

Acknowledgement: The authors gratefully acknowledge the financial support of CAPES and CNPq (Brazil), which made this research possible.

References

Abdo, M. A.-B.; Hori, M. (2002): A numerical study of structural damage detection using changes in the rotation of mode shapes. In: *Journal of Sound and Vibration*, 251(2), pp. 227-239.

Adams, R. D.; Cawley, P.; Pye, C. J.; Stone B. J. (1978): A vibration technique for nondestructively assessing the integrity of structures. In: *Journal of Mechanical Engineering Science*, 20(2), pp. 93-100.

Bazant, Z. P.; Sener, S.; Prat, P. C. (1987): Size effect test of failure of plain and reinforced concrete beams. In: *Materials and Structures*, 21(2), pp. 425-430.

Bazant, Z. P.; Kazemi, M. T. (1989): Size effect on diagonal shear failure of beams without stirrups. In: *Report 89-8/498S, Center for Advanced Cement-Based Materials*, Northwestern University, Evanston.

Bosco, C.; Carpitineri, A.; Debernardi, P. G. (1990): Minimum reinforcement in high-strength concrete. In: *Journal of Structural Engineering*, 16(2), pp. 427-437.

Brasiliano, A. (2001): Caracterização de danos em estruturas aporticadas. *Master Thesis*, Department of Civil and Environmental Engineering, University of Brasília, Brasília, DF, Brazil.

Brasiliano, A.; Doz, G. N.; Brito, J. L. V. (2004): Damage identification in continuous beams and frame structures using the Residual Error Method in the Movement Equation. In: *Nuclear Engineering and Design*, 227(1), pp. 1-17.

CEB-FIB (1990): *Model Code for Concrete Structures*, pp. 33-37.

Chen, H. L.; Spyrakos, C. C.; Venkatesh, G. (1995): Evaluating structural deterioration by dynamic response. In: *Journal of Structural Engineering*, 121(8), pp. 1197-1203.

Doebling, S. W.; Farrar, C. R.; Prime, M. B. (1998): A summary review of vibration-based damage identification methods. In: *The Shock and Vibration Digest*, 30(2), pp. 91-105.

Doz, G. N.; Riera, J. D. (2000): Towards the numerical simulation of the seismic excitation,. In: *Nuclear Engineering and Design*, 196, pp. 253-261.

Du, J.; Yon, J. H.; Hawkins, N. M.; Arakawa, K.; Kobayashi, A. S. (1992): Fracture process zone for concrete for dynamic loading. In: *ACI Materials Journal*, 89(3), pp. 252-258.

Genovese, M. (2000): Localização e quantificação de danos em estruturas por meio de suas características dinâmicas. *Master Thesis*, PPGEC, University of Brasília, Brasília, Brazil.

Genovese, M. (2005): Avaliação estrutural: Influência do ruído nos métodos de detecção de danos baseados na análise das propriedades dinâmicas. *DSc Thesis*, PPGEC, University of Brasília, Brasília,, Brazil.

Griffith, A. A. (1921): The phenomena of rupture and flaw in solids. In: *Transactions Royal Society of London*, A221, pp. 163-198.

Gudiel, L. A. D.; Irikura, K.; Riera, J. D.; Chiu, H.C. (2003): Simulation of tensile crack generation by three-dimensional dynamic shear rupture propagation during an earthquake. In: *Journal of Geophysical Research*. 108(B3), pp. 1-21.

Gudiel, L. A. D. (2000): Simulação de Movimento Sísmico Considerando o Mecanismo de Ruptura da Falha Causativa do Terremoto. *DSc Thesis*, CPGEC, Federal University of Rio Grande do Sul, Porto Alegre, Brazil

Hayashi, Y. (1982): Sobre uma representação discreta de meios contínuos em dinâmica nãolinear. *Master Thesis*, CPGEC, Federal University of Rio Grande do Sul, Porto Alegre, Brazil.

Hearn, G.; Testa, R. B. (1991): Modal analysis for damage detection in structures. In: *Journal of Structural Engineering*, 117(10), pp. 3042-3063.

Irwin, G. R. (1958): Fracture. In: *Handbach der Phisik*, Vol. VI, Flugge, Springer, pp. 551-590.

Iturrioz, I. (1995): Aplicação do método dos elementos discretos ao estudo de estruturas laminares de concreto armado. *DSc. Thesis*, CPGEC, Federal University of Rio Grande do Sul, Porto Alegre, Brazil.

Kaplan, M. F. (1961): Crack propagation and the fracture of concrete. In: *ACI Journal*, 58(5), pp. 591-610.

Nayfeh, A. H.; Hefzy, M. S. (1978): Continuum modelling of three-dimensional truss-like space structures. In: *AIAA Journal*, 16(8), pp. 779-787.

Ndambi, J.-M.; Vantomme, J.; Harri, K. (2002): Damage assessment in reinforced concrete beams using eigenfrequencies and mode shapes derivatives. In: *Engineering structures*, 24, pp. 501-515.

Petersson, P. E. (1981): Crack growth and development of fracture zones in plain concrete and similar materials. In: *Report TVBM-1006*, Lund, Sweden.

Rios, R. D.; Riera, J. D. (2002): Consideração do efeito de escala em estruturas de concreto. In: Anais das XXX Jornadas Sul-Americanas de Engenharia Estrutural, Brasília, Brazil.

Rocha, M. M. (1989): Ruptura e efeitos de escala em materiais não-homogêneos. *Master Thesis*, CPGEC, Federal University of Rio Grande do Sul, Porto Alegre, Brazil.

Salawu, O. S. (1997): Detection of structural damage through changes in frequency: a review. In: *Engineering Structures*, 19(9), pp. 718-723.

Saleh, A. L.; Aliabadi, M. H. (1998): Crack growth analysis in reinforced concrete using BEM. In: *Journal of Engineering Mechanics*, 124(9), pp. 949-958.

Souza, W. R. M. (2001): Propagação de fissuras em vigas submetidas a diferentes estados de carregamento. *Master Thesis*, Department of Civil and Environmental Engineering, University of Brasília, Brasília, DF, Brazil.

Swartz, S.; Taha, N. M. (1991): Crack propagation and fracture of plain concrete beams subjected to shear and compression. In: *ACI Structural Journal*, 88(2), pp. 169-177.

Zou, Y.; Tong, L.; Steven, G. P. (2000): Vibration-based model-dependent damage delamination identification and health monitoring for composite structures – A Review. In: *Journal of Sound and Vibration*, 230(2), pp. 357-378.